Supplementary information

Optically intensity-driven reversible photonic bandgaps in self-organized helical superstructures with handedness inversion

Jian Sun,[a] Li Yu,[b] Ling Wang,[b] Chenyue Li,[a] Zhou Yang,[a] Wangli He,[a] Cuihong Zhang,[b] Lanying Zhang,[be] Jiumei Xiao,[c] Xiao Yuan,[b] Fasheng Li[d] and Huai Yang*[abe]

[a] Department of Materials Science and Engineering, University of Science and Technology Beijing, Beijing 100083, China.
[b] Department of Materials Science and Engineering, College of Engineering, Peking University, Beijing 100871, China.
[c] School of Mathematics and Physics, University of Science and Technology Beijing, Beijing 100083, China.
[d] College of Medical Laboratory, Dalian Medical University, Dalian 116044, China.
[e] Key Laboratory of Polymer Chemistry and Physics of Ministry of Education, Peking University, Beijing 100871, China.

Content

1. Experimental details

All starting materials, solvents and reagents were commercial products and used without further purification. Column chromatography was performed using silica gel (200-300 mesh) and thin-layer chromatography (TLC) was carried out on aluminum sheets coated with silica 60 F254 obtained from Merck. ^{1}H and ^{13}C spectra were recorded on Varian 300 MHz and Bruker 400 MHz spectrometer. Chemical shifts (δ) are denoted in parts per million (ppm) relative to tetramethylsilane (TMS) (for ^{1}H detection, $\delta = 0.00$ ppm; for ^{13}C detection, $\delta = 0.00$ ppm) and $CDCl_3$ (for ^{1}H detection, $\delta = 7.26$ ppm; for ^{13}C detection, $\delta = 77.16$ ppm). For ^{1}H NMR spectroscopy, the splitting pattern of peaks is designated as follow: s (singlet), d (doublet), t (triplet), m (multiplet), br (broad), or dd (doublet of doublets). The spectra of absorption and transmission were obtained with a UV/VIS/NIR spectrophotometer (Lambda 950, Perkin Elmer). The right-handed and left-handed circularly polarized (RCP and LCP) transmittance spectra are detected by setting a Glan Thompson polarizer (350-2300 nm) and an achromatic quarter-wave plate (450-650 nm, 650-1100 nm, 900-2300 nm) in the light path of the spectrophotometer. Textures and disclination line in Grandjean-Cano wedge cell (KCRK-07, tan θ = 0.0196, EHC) were observed by polarized optical microscopy (POM, Axio Scope A1 pol, Zeiss). The microstructure of the gel film was observed by scanning electron microscopy (SEM, Hitachi S4800). The UV light (365 nm) irradiation was carried out with a LED lamp (FUV-6BK, Bangwo Elec. Technologies Co., Ltd.). In order to prevent out-of-plane rotation of the CLC molecules in photo-tuning and dark relaxation, a negative dielectric anisotropy nematic liquid crystal was

used and a square-wave-modulated electric field (1.5 $V\mu m^{-1}$, 2.0 kHz) was applied across the cell. The infrared thermal images were obtained with Thermal Infrared Imager (UTi160B, Uni-Trend Technology Limited).

2. Synthesis and characterizations of chiral overcrowded alkene M1

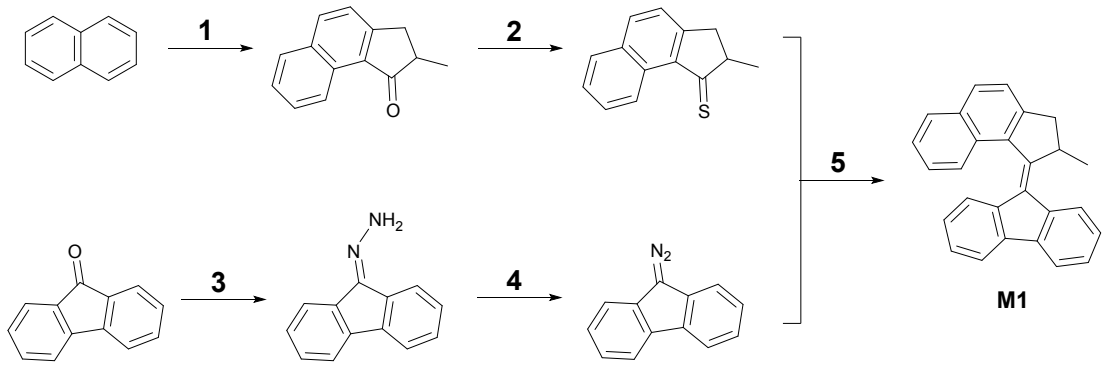

Scheme S1. Synthesis of photo-driven chiral overcrowded alkene molecule **M1**. Reagents and conditions: (1) MAA, PPA, 110 °C; (2) Lawsson's reagent, toluene, 90 °C, reflux; (3) $H_2NNH_2 \cdot H_2O$, EtOH, 85 °C, reflux; (4) activity MnO_2, $MgSO_4$, CH_2Cl_2; (5) PPh_3, toluene, 90 °C, reflux.

Characterization data for M5: ^{1}H NMR (400 MHz, $CDCl_3$): δ = 8.01 (dd, J = 5.6, 3.2 Hz, 1H), 7.94 (t, J = 8.9 Hz, 2H), 7.87 (dd, J = 5.6, 3.1 Hz, 1H), 7.78 (dd, J = 7.9, 4.7 Hz, 2H), 7.59 (d, J = 8.2 Hz, 1H), 7.48 (t, J = 7.4 Hz, 1H), 7.41 (m, 2H), 7.34 (t, J = 7.6 Hz, 1H), 7.23 (t, J = 7.4 Hz, 1H), 6.82 (t, J = 7.3 Hz, 1H), 6.74 (d, J = 7.9 Hz, 1H), 4.46 – 4.27 (m, 1H), 3.59 (dd, J = 15.0, 5.6 Hz, 1H), 2.78 (d, J = 15.0 Hz, 1H), 1.40 (d, J = 6.7 Hz, 3H); ^{13}C NMR (100 MHz, $CDCl_3$): δ = 151.19, 147.47, 140.15, 139.88, 139.61, 137.18, 136.42, 132.69, 130.92, 130.50, 129.89, 128.72, 127.57, 126.98, 126.94, 126.63, 125.94, 125.36, 124.10, 124.05, 119.73, 119.00, 45.57, 42.03, 19.36.

Chiral resolution of **M1** was achieved by preparative HPLC, using a chiral ChiralCN OD column (Guangzhou Research & Creativity Biotechnology Co., Ltd.) in hexane:

EtOH (97.0: 3.0), the enantiomeric excess (*e.e.*) = 98.8%.

3. Characterization of reversible chiral overcrowded alkene M1

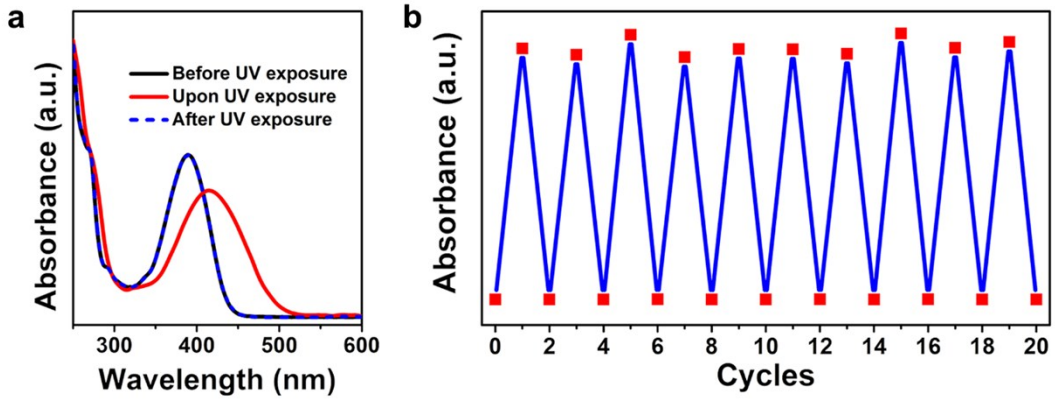

Figure S1. (a) Change in UV-vis absorption spectra of **M1** in CH_2Cl_2 (20 μg/mL) before, upon and after UV light (365 nm, 2.0 mW cm^{-2}) exposure at room temperature. (b) Cycles of absorbance of **M1** in CH_2Cl_2 (20 μg/mL) at 450 nm as the solution was irradiated with UV light for 2 minutes and then relaxed in the dark for 20 minutes repeatedly.

4. Production of photoresponsive CLCs and PSCLCs

Chiral overcrowded alkene, **M1** (initially right-handed)

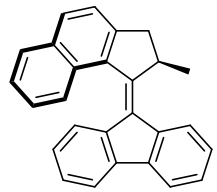

Photo-polymerizable liquid crystal monomer, **C6M**

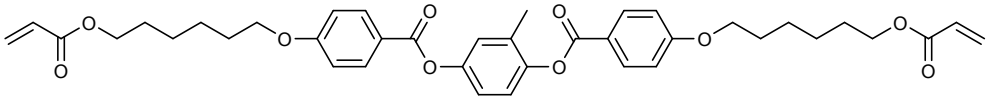

Photo-initiator, **Irg 651**

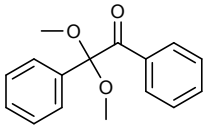

Figure S2. Chemical structures of components used in the photoresponsive CLC mixtures.

The photoresponsive CLC mixtures were fabricated by doping M1 (initially RH) with different content in a commercial nematic liquid-crystal mixture SLC10V513 (LC513; n_e = 1.698, Δn = 0.15; Slichem).

The materials used to produce the PSCLC films are shown in Figure S2. As the foundation of the photo-thermal effect and the photodynamic respond time to the photoresponsive CLCs mentioned in the main text, the PSCLC films were fabricated using a mixture containing 3.5 or 8.0 wt% **M1**, 20.0 wt% **C6M**, 1.0 wt% **Irg651** in LC513. Photo-polymerization was initiated by UV light (365 nm) for 30 minutes at room temperature.

For SEM characterization, the PSCLC sample was quick-frozen to crystallize the CLC molecular alignment by liquid nitrogen and then the frozen section was immediately

cut off. The fractured surface of the PSCLC was coated with a thin layer of gold to eliminate any electric charge problem.

5. UV light induced handedness inversion of photoresponsive CLC upon exposure to different intensities

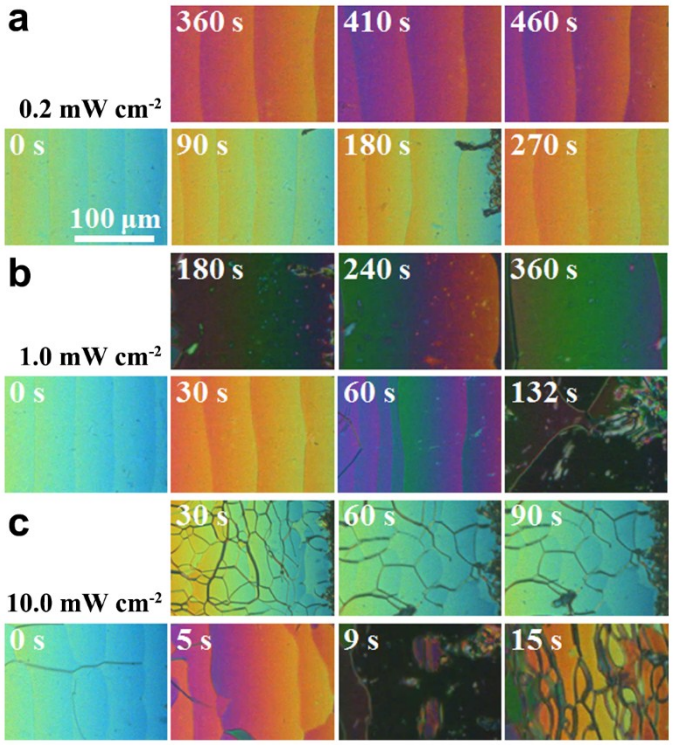

Figure S3. Handedness inversion behavior of CLC mixture (1.0 wt% **M1** in LC513) in the wedge cell exposure upon UV light at (a) 0.2, (b) 1.0 and (c) 10.0 mW cm^{-2} observed by a transmission-mode POM.

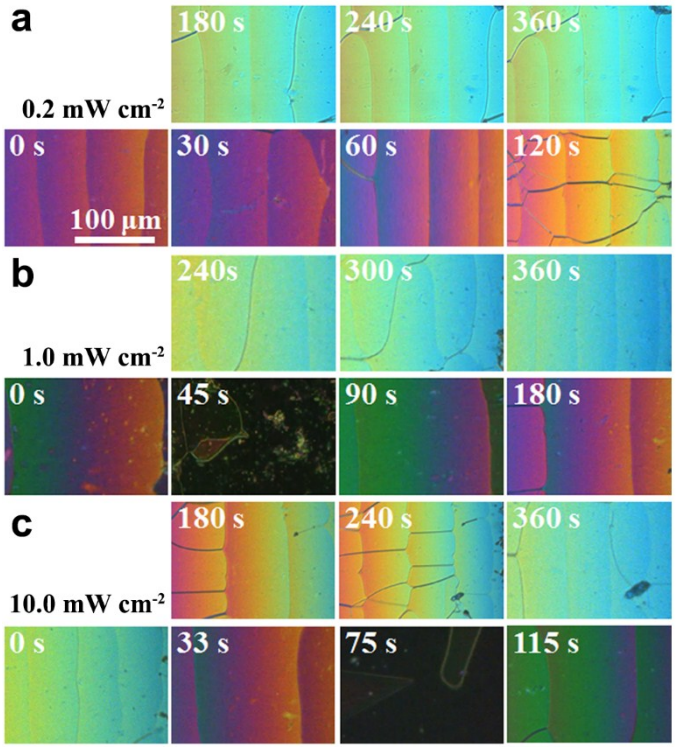

Figure S4. Handedness inversion behavior of CLC mixture (1.0 wt% **M1** in LC513) in the wedge cell after ceasing UV light irradiation at (a) 0.2, (b) 1.0 and (c) 10.0 mW cm^{-2} observed by a transmission-mode POM.

6. Photo-tuning and relaxation behaviors of the photoresponsive CLCs

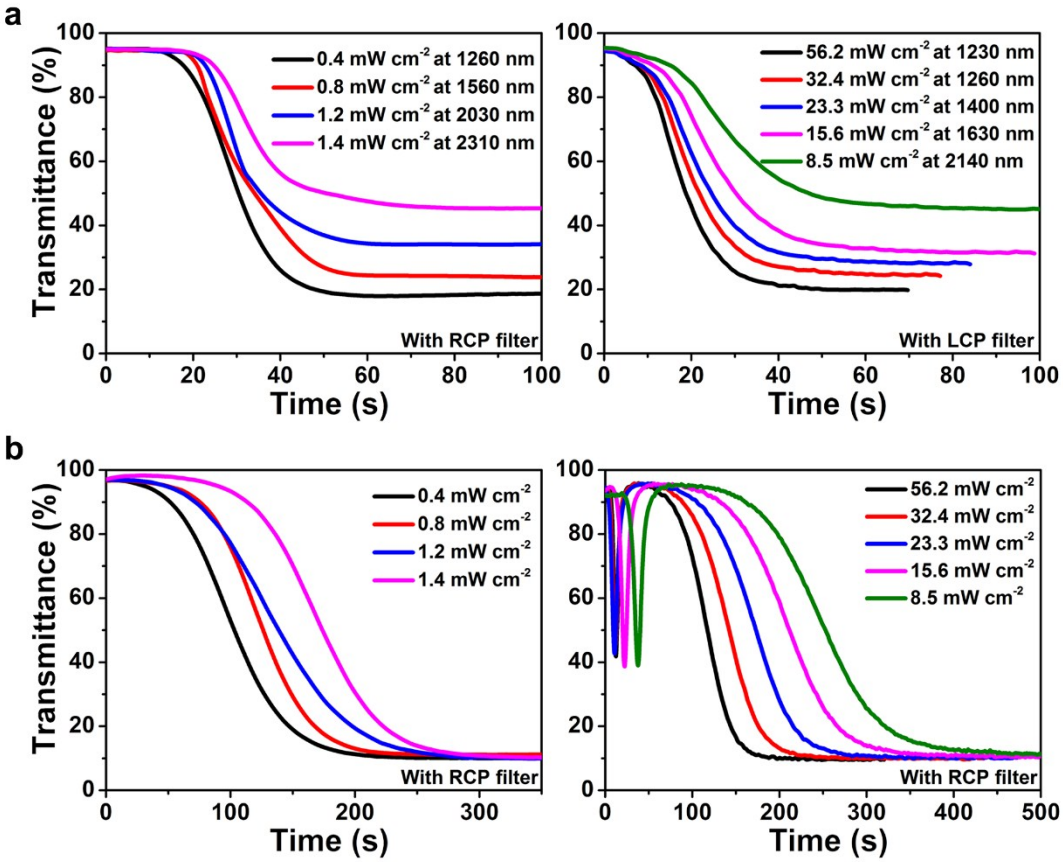

Figure S5. The transmittance changes of CLC (3.5 wt% **M1** in LC513) in 10 μm cell during (a) photo-tuning at λ_{PSS} under different UV-exposure intensities with RCP and LCP filter and (b) relaxing helix conversion at the original reflection wavelength (1030 nm) in the dark with RCP filter.

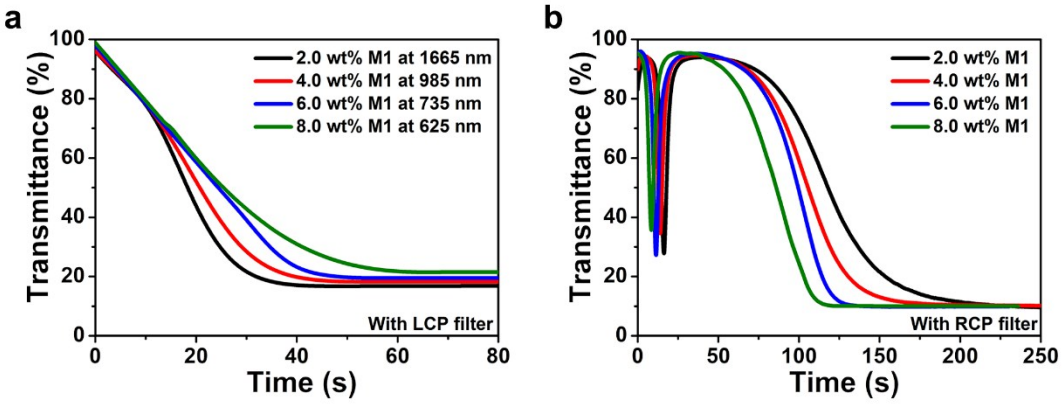

Figure S6. The transmittance changes of CLC (2.0 to 8.0 wt% **M1** in LC513) in 10 μm cell during (a) photo-tuning at λ_{PSS} upon UV exposure (56.2 mW cm^{-2}) with LCP filter and (b) relaxing helix conversion at the original reflection wavelength (1030 nm) in the dark with RCP filter.

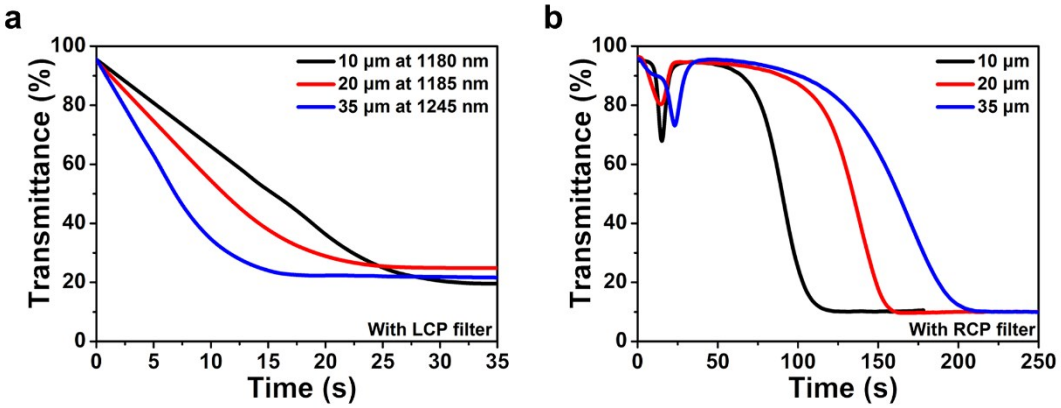

Figure S7. The transmittance transmittance changes of CLC (3.5 wt% **M1** in LC513) in 10, 20 and 35 μm cell during (a) photo-tuning at λ_{PSS} upon UV exposure (74.0 mW cm^{-2}) with LCP filter and (b) relaxing helix conversion at the original reflection wavelength (1030 nm) in the dark with RCP filter.

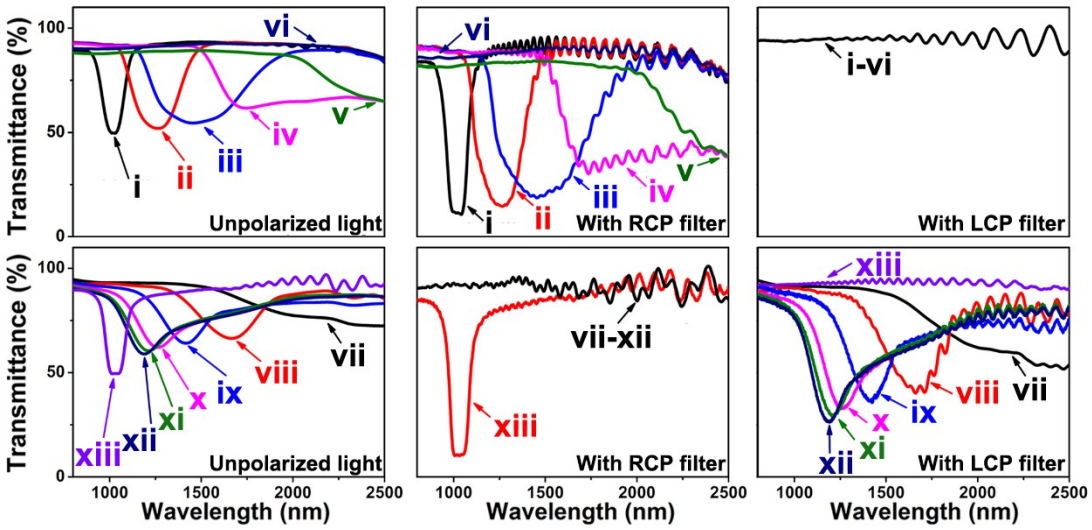

Figure S8. The unpolarized, RCP and LCP transmittance spectra of CLC (3.5 wt% **M1** in LC513) exposed to UV light (i) 0.0, (ii) 0.5, (iii) 0.9, (iv) 1.8, (v) 3.1, (vi) 4.9, (vii) 14.5, (viii) 23.3, (ix) 32.4, (x) 42.2, (xi) 56.2, (xii) 74.0 mW cm^{-2} and (xiii) after UV curing in 20 μm cell. Schematic illustrations of the photo-tuning CLC exposed to 0.9 mW cm^{-2} UV light in right panel.

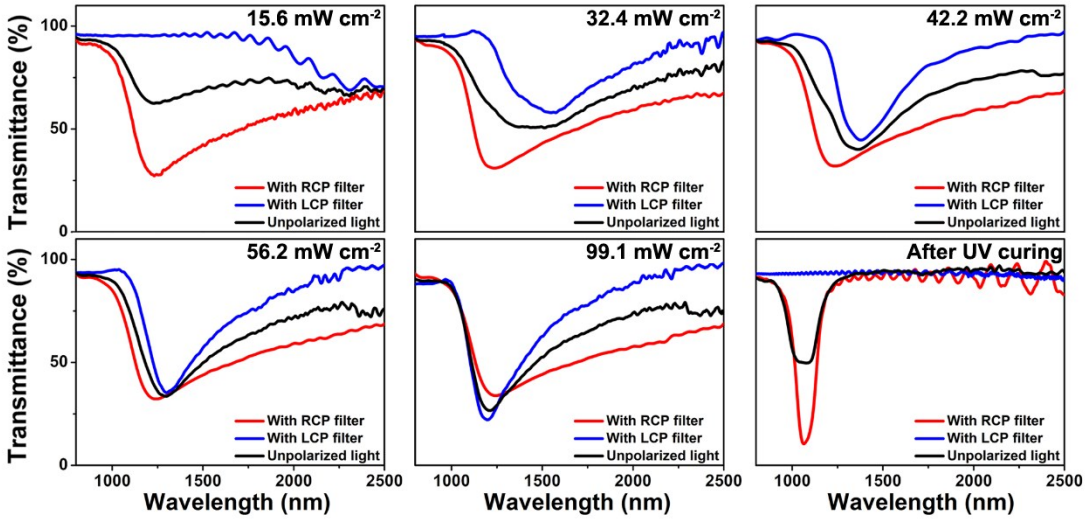

Figure S9. The unpolarized, RCP and LCP transmittance spectra of CLC (3.5 wt% **M1** in LC513) exposed to UV light (15.6, 32.4, 42.2, 56.2 and 99.1 mW cm^{-2}) and after UV curing in 35 μm cell.

7. Photothermal effect of the photoresponsive CLCs

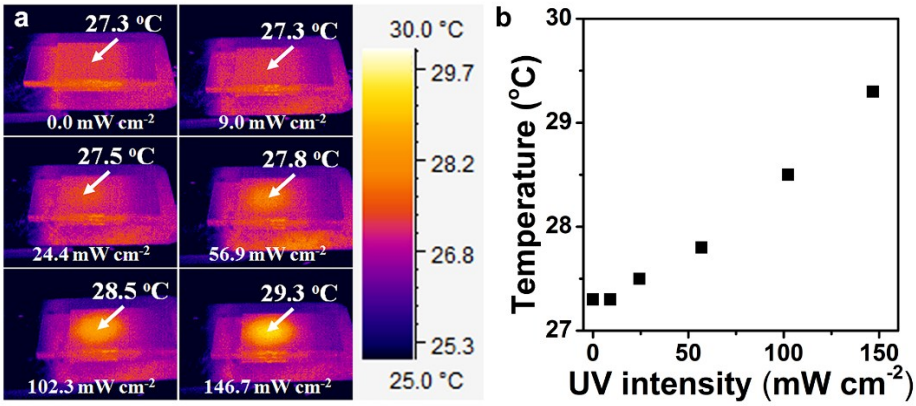

Figure S10. (a) The infrared thermal images of CLC (3.5 wt% M1 in LC513) upon UV exposure of different intensity. (b) Plots of temperature change for different UV intensity (0.0-146.7 mW cm^{-2}) irradiation with CLC.

8. The transmittance spectra of the PSCLCs

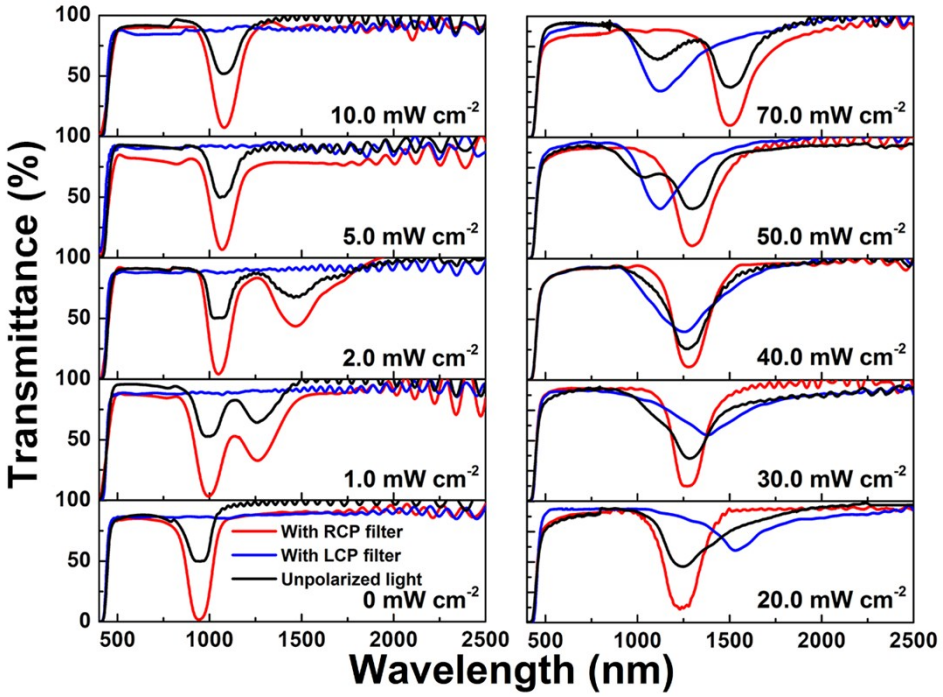

Figure S11. The unpolarized, RCP and LCP transmittance spectra of 20 μm PSCLC with different UV photopolymerization intensity (0.0-70.0 mW cm^{-2}), respectively.

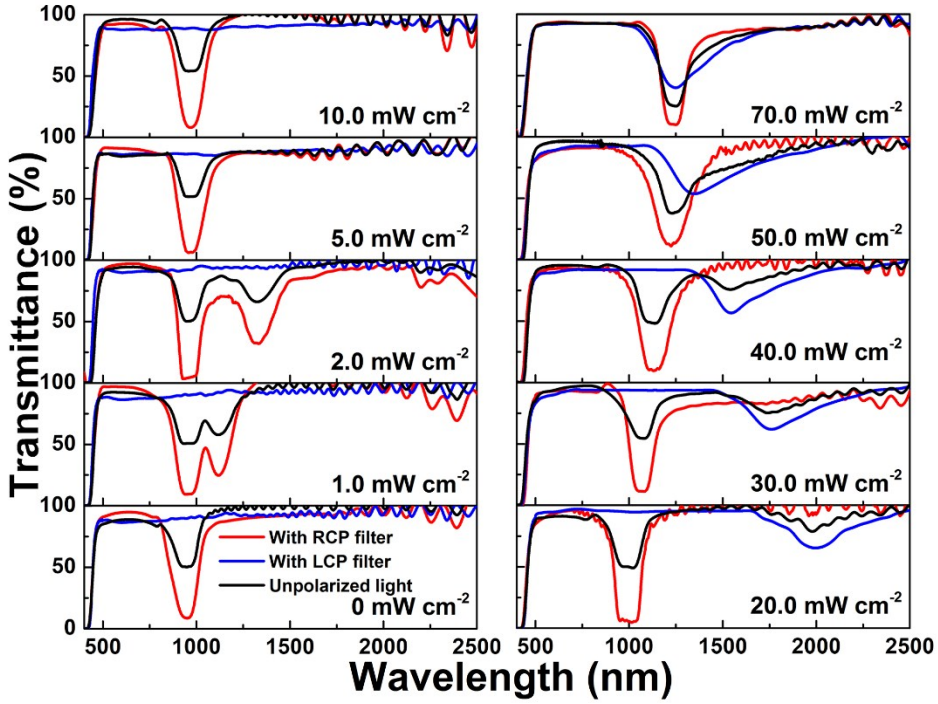

Figure S12. The unpolarized, RCP and LCP transmittance spectra of 35 μm PSCLC with different UV polymerization intensity (0.0-70.0 mW cm^{-2}), respectively.

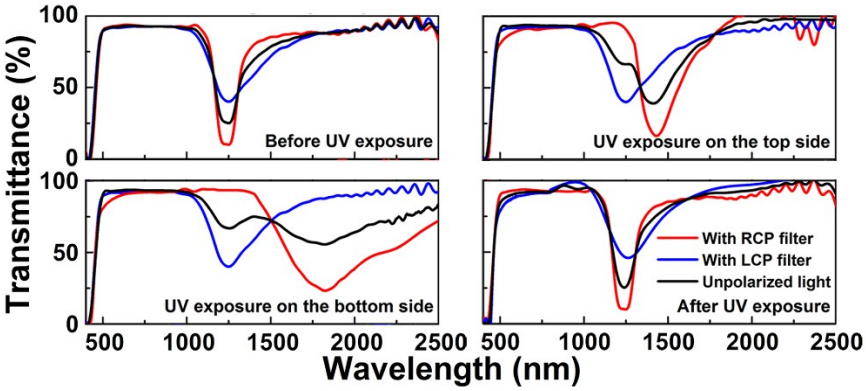

Figure S13. The unpolarized, RCP and LCP transmittance spectra of 35 μm PSCLC before and after being modulated by UV exposure with 3.5 mW cm^{-2} on the top side and the bottom side.

9. ^{1}H and ^{13}C NMR spectra of M1 in $CDCl_3$

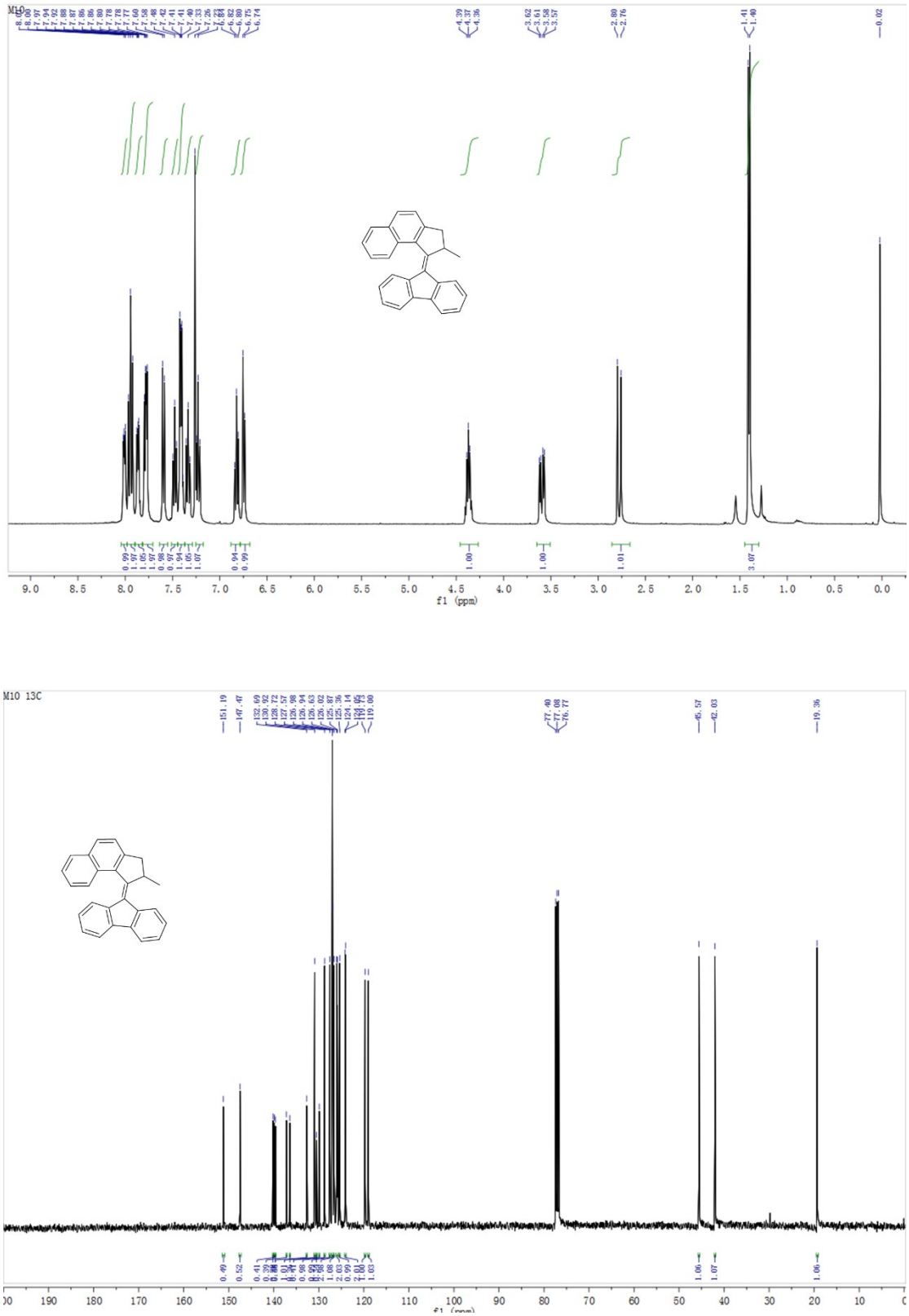

Figure S14. ^{1}H and ^{13}C NMR spectra of **M1** in $CDCl_3$